Distribution Agreement

In presenting this thesis as a partial fulfillment of the requirements for a degree from Emory University, I hereby grant to Emory University and its agents the non-exclusive license to archive, make accessible, and display my thesis in whole or in part in all forms of media, now or hereafter now, including display on the World Wide Web. I understand that I may select some access restrictions as part of the online submission of this thesis. I retain all ownership rights to the copyright of the thesis. I also retain the right to use in future works (such as articles or books) all or part of this thesis.

Somin Kim March 25, 2018

Investigating the role of epigenetics in the development of myopia and retinal degeneration in the interphotoreceptor retinoid-binding protein deficient mouse model

by

Somin Kim

Dr. John Nickerson
Adviser

Biology Department

Dr. John Nickerson

Adviser

Dr. Arri Eisen

Committee Member

Dr. Davide Fossati

Committee Member

2019

Investigating the role of epigenetics in the development of myopia and retinal degeneration in the interphotoreceptor retinoid-binding protein deficient mouse model

By

Somin Kim

Dr. John Nickerson

Adviser

An abstract of
a thesis submitted to the Faculty of Emory College of Arts and Sciences
of Emory University in partial fulfillment
of the requirements of the degree of
Bachelor of Sciences with Honors

Biology Department

2019

Abstract

Investigating the role of epigenetics in the development of myopia and retinal degeneration in the interphotoreceptor retinoid-binding protein deficient mouse model

By Somin Kim

Little is known about the role of histone modifying proteins in the development of myopia and retinal degeneration (RD). Here we begin to phenotypically characterize the effects of histone deacetylase inhibitors (HDACi) Trichostatin-A (TSA) and Valproic Acid (VPA) in an interphotoreceptor retinoid-binding protein (IRBP) knockout (KO) mouse model, a model known to rapidly induce myopia and retinal degeneration in mice. To determine how these HDACi impacts these deteriorating eye conditions, we randomly assigned IRBP KO mice to experimental and control groups. In the TSA condition, mice were injected daily with TSA (2.5mg/kg) or vehicle (10% DMSO) intraperitoneally using a double-blind system over the course of 5 days. In the VPA condition, mice were injected daily with VPA (350mg/kg) or vehicle (1XPBS) intraperitoneally using a double-blind system over the course of 5 days. Whole-eye biometry was utilized to observe retinal layers, and electroretinography (ERG) was performed to provide additional information regarding how retinal function is affected, both of which showed that the chosen dosage of VPA or TSA made no significant improvement to visual function or the myopic phenotype. TSA (1mg/kg) was further tested for its preventative effects in young mice IRBP KO mice, yet again no improvement in retinal morphology or function could be detected following treatment. Immunofluorescence, enzymatic assays, and western blots were conducted to reveal endogenous levels of HDAC3 deacetylate activity in IRBP KO mice as grounds for a possible underlying mechanism but was revealed that the absence of IRBP does not affect HDAC3 activity or quantity. Data from these experiments will provide critical information on what role epigenetics plays in myopia and RD and the importance IRBP plays in the normal development of the eye.

Investigating the role of epigenetics in the development of myopia and retinal degeneration in the interphotoreceptor retinoid-binding protein deficient mouse model

By

Somin Kim

Dr. John Nickerson

Adviser

A thesis submitted to the Faculty of Emory College of Arts and Sciences
of Emory University in partial fulfillment
of the requirements of the degree of
Bachelor of Sciences with Honors

Biology Department

2019

Acknowledgements

I would like to thank Dr. Shanu Markand and Salma Ferdous for their mentorship, and of course my amazing PI Dr. John Nickerson for his continuous support and advice. I additionally would like to thank my other committee members, Dr, Arri Eisen and Dr. Davide Fossati, for taking the time to mentor me through this process. Research was funded in part by Research to Prevent Blindness.

Table of Contents

Introduction

Myopia is the most common human eye disorder in the world, with 85-90% of young adults in several Asian countries and 25-50% of older adults in the western hemisphere being affected (Wu, 2016). The disorder is characterized by the elongation of the eyeball resulting in light focusing at a point in front of the retina rather than directly on the retinal surface. Due to this refraction error, distant objects appear out of focus in myopia and thus current approaches to control myopia include glasses, contact lenses, and refractive surgery (Leo, 2017). The prevalence and incidence rate of myopia has rapidly increased over the past decade (Hornbeak and Young, 2009) and the development of myopia can lead to more serious conditions such as retinal degeneration and glaucoma (Dolgon, 2015). Current understanding of the mechanisms behind myopia development are lacking and therefor provide cause for further investigation.

Not only are the underlying mechanism of myopia unclear, but also few studies have interrogated the role of epigenetics in myopia. Epigenetics is the alteration in gene expression due to changes in the environment, independent of changes in genome sequence. The studies that do investigate epigenetic roles argue that as external ocular tissues are exposed to the outside environment such as light, the eye is a sustainable model organ for epigenetic studies. Many currently available studies have focused on non-coding RNAs and DNA methylation, both of which have been found to be involved in the progression of myopia (Chen et al., 2012; Zhou et al., 2012). It is becoming clearer that epigenetics plays an important role in the development of the eye. However, the understanding of other epigenetic factor roles, specifically the role of HDACs (proteins involved in the removal of acetyl groups from lysine amino acids on histones, often allowing the histone to wrap the DNA more tightly), in the mechanisms of myopia is scarce.

One of the primary focuses of our laboratory is to understand the role of interphotoreceptor retinoid-binding protein (IRBP) in normal eye development. IRBP is a major protein of the sub-retinal space and plays a crucial role in the visual cycle (Pepperberg et al., 1993). In the normal mouse eye, much of its development, including differentiation of virtually all retinal cells, occurs from postnatal day 1 (P1) to postnatal day 13 (P13), while the eye has yet to open. Our laboratory has previously reported eye size defects starting at P7 with profound myopia and onset of retinal degeneration by P23 in IRBP knockout (IRBP KO) mice, indicating a role for IRBP in normal eye development and the pathogenesis of myopia. Total axial length and vitreous chamber depth are significantly increased in IRBP KO mice, with eye weights of IRBP KO mice beginning to deviate at P7 (Figure 1A). *In-vivo* whole-eye biometrical spectral domain optical coherence tomography (SD-OCT) data analysis in C57BL/6J (C57 WT) and IRBP KO showed loss of total retina thickness and photoreceptor thickness (Figure 1B), but no significant difference in other morphologies (Markand et al., 2016). While this research has produced promising data, the exact mechanisms underlying myopia and retinal degeneration in IRBP KO mouse are not yet clear. However, epigenetic factors seem to be a likely contributor in the IRBP KO mouse model as they are primary regulators of gene expression. Independence from vision-dependent refractive growth in IRBP KO mice makes this model particularly interesting to investigate in regard to epigenetics.

We have shown that IRBP is important in normal eye development and emmetropization, but the underlying mechanisms are not clear. Additionally, amelioration of retinal degeneration (RD) or myopia by a pharmacological approach has not been investigated previously in IRBP KO mice. The current study examines a novel epigenetic mechanism associated with IRBP-mediated myopia and RD. Trichostatin-A (TSA) selectively inhibits class

I and class II histone deacetylates. It has been previously shown that the inhibition of HDAC class I/II activity strongly reduces photoreceptor cell death (Sancho-Pelluz et al., 2010). TSA has also been shown to protect against retinal thinning at 7 days post- ischemia/reperfusion, in addition to having the functional benefit of attenuating the loss of a- and b-wave amplitude (Crosson et al., 2010). TSA is our primary drug candidate not only because of its relevant protective effects and ready accessibility, but also due to its possible clinical applications, as it is structurally related to one of the three FDA approved HDAC inhibitors, Vorinostat (Mottamal et al., 2015). **Based on these studies, we hypothesize that the addition of an HDAC inhibitor to our IRBP KO mouse model will slow the development of myopia and rescue retinal layers.**

In addition to TSA, Valproic acid (VPA) is another example of a histone deacetylase inhibitor (HDACi) that we wish to test—although it is most commonly used in neurological settings, several studies have investigated its treatment potential for a myriad of ocular damage disorders. VPA has been shown to have anti-apoptotic properties and prevent photoreceptor loss (Mitton et al., 2014), which is of interest to our study as in our IRBP KO mice we see a burst of apoptosis occur in the outer nuclear layer (ONL) peaking at P25, killing 40% of the photoreceptors in less than a week and, thereafter, photoreceptor cell death continues gradually as the KO mouse ages (Wisard et al., 2011). Additionally, it has been shown that VPA can prevent retinal ganglion cell death and thinning of the inner retinal layer in a glaucoma (Kimura et al., 2015). Valproic acid has also been used in clinical trials to treat retinitis pigmentosa, showing that VPA administered to patients at 500mg/kg caused an improvement to their visual fields (Clemson et al., 2009). We wish to examine the effects of VPA in IRBP KO mice, as we believe the beneficial effects of VPA shown in other models can apply to myopia and RD as well. **Our hypothesis is that the aberrant imbalance in**

histone acetylation and deacetylation enzymes contributes to the ocular phenotype in IRBP KO mice and administration of valproic acid will ameliorate RD and myopia in IRBP KO mice.

Collectively, our proposed study will advance our understanding of the etiology of IRBP-mediated myopia and retinal degeneration. Our study is novel—light-independent epigenetic mechanisms of myopia have not yet been studied. Data from these experiments will contribute to our understanding of the importance of IRBP in the normal development of the eye.

Results

Endogenous HDAC3 activity and protein quantity remain unchanged in IRBP KO mice

To better understand the endogenous epigenetic profile of IRBP KO mice, Retinal protein was extracted from P40 IRBP KO/KO (n=4) and C57 mice (n=4). An HDAC3 enzymatic assay kit was performed on the isolated protein and yielded the result that IRBP KO/KO mice did not have significantly less HDAC3 enzymatic activity than corresponding controls (unpaired t-test) (Figure 3A). To connect enzymatic activity with protein quantification, immunofluorescence was conducted on P36 IRBP KO/KO and C57 eye sections. No obvious difference could be seen between sections, nor could fluorescence analysis detect a statistical change (unpaired t-test) (Figure 3B). To validate IHC results, western blotting for HDAC3 (17kDa) was done on P70 IRBP KO/KO and C57 isolated retinal protein. No significant differences were observed (Figure 3C).

H3k9me^3 expression is unaffected by the absence of IRBP

As histone acetylation was unchanged in IRBP KO mice, another common histone modification, methylation, was investigated for any changes in regulation. Immunofluorescence staining for H3k9me^3, a well-known histone methylation marker, was conducted on P5 and P36

IRBP KO and C57 eye sections. Fluorescence quantification showed no significant differences between ages, or within strains, in regards to the presence of H3k9me^3 expression in retinal tissue (Figure 4A, 4B). It is interesting to note that H3k9me3 becomes less prevalent in P36 mice lens. The severity of the myopic phenotype in older IRBP KO mice can clearly be seen in the much more elongated P36 IRBP KO eye (Figure 4B).

HDAC inhibitor Trichostatin-A is not protective in a significantly myopic model

With the goal of determining a potential pharmacological role for TSA in a significantly myopic mouse model, as well as establishing non-lethal drug dosage, IRBP KO/KO and C57 WT were injected intraperitoneally with TSA (2.5mg/kg) daily over the course of 5 days starting from P40 (non-injected mice were also kept for naive controls). Whole-eye biometry was performed on IRBP KO/KO (n=2) and C57 WT (n=2) both before and after injection of either TSA of vehicle. There was no significant difference in either total axial length or retinal thickness following treatment of TSA in IRBP KO mice (paired t-test), but there continued to be significantly decreased retinal thickness and increased total axial length in IRBP KO mice (unpaired t-test) (Figure 5A). Additionally, TSA was not preventative of cone-driven vision loss in IRBP KO/KO mice. Both photoreceptors (a-wave) and ON bipolar cells (b-wave) continued to decrease in function despite treatment with TSA (unpaired t-test between C57 WT and IRBP KO/KO groups). Paired t-tests revealed no significance between differences in IRBP KO/KO and IRBP KO/KO + TSA conditions (Figure 5D).

HDAC inhibitor Valproic Acid is not protective in a severely myopic and retinal degenerative model

To experimentally explore the effect VPA may have on myopia and retinal degeneration in an older mouse model, as well as determining an effective drug dosage, IRBP KO/KO and

were injected intraperitoneally with VPA (350mg/kg) or vehicle (1XPBS) daily over the course of 5 days starting from P40. SD-OCT was performed on IRBP KO mice (n=4) 3 days after injection and 30 days after injection of either VPA or vehicle. There was no significant difference in retinal thickness following treatment of VPA in IRBP KO/KO mice (unpaired t-test). No significant difference was exhibited between 3 days and 30 days after injection measurements either (paired t-test). Additionally, no significant difference was observed in photoreceptor thickness between VPA and vehicle injected IRBP KO/KO mice (Figure 6A). Whole-eye biometry data collected pre-injection, 3 days post-injection, 10 days post-injection, and 25 days post-injection from IBRP KO mice treated with either VPA (n=4) or vehicle (n=4) revealed that although with passing time IRBP KO mice continue to become more myopic (characterized by an increase in total axial length of the eye), no significant changes in morphology could be detected in axial length between the VPA treated and vehicle treated mice at each time point (unpaired t-test) (Figure 6C).

ERG data was also collected on injected IBRP KO mice (n=4) both pre-injection (P37) and post-injection (P58) in order to test for retention of visual function. Similarly to TSA, no significant changes could be detected in between VPA injected mice and vehicle injected mice both before injection and after injection (Figure 6D).

Trichostatin A has no effect in young IRBP KO mice

In order to test the preventative effects TSA may have on retinal degeneration, P7 IRBP KO pups were injected with either TSA (1mg/kg) (n=4) or vehicle (5% DMSO) (n=4) daily over the course of 7 days intraperitoneally. A non-injected group (n=3) was included for control. As pup's eyes are not suitable for *in vivo* imaging or experimentation until P25, post-injection data was collected much later at P70. Whole-eye biometry and ERG data was collected at P70 and

both tests revealed that although there was less axial lengthening observed in the TSA injected group compared to the non-injected group, no significant differences in eye morphology (Figure 7A) or retinal function (Figure 7B) across the different treatment groups.

Discussion

As myopia is such a prevalent condition across the globe, it is of significant interest to find treatments to counteract severe myopia and retinal degeneration. The aim of this study was to conduct comprehensive analyses on the effect of TSA and VPA on myopia and RD in the myopic IRBP KO mouse model.

The present study first took both a quantitative and qualitative approach to determining endogenous levels of HDAC protein present in IRBP KO and C57 WT control mouse retina. An HDAC3 enzymatic assay was performed to assess HDAC3 activity level within the retina. When no statistical differences in activity were observed, a western blot and IHC assay were performed to see whether the difference in activity was due to a difference in protein location and quantity. There was no difference observed in protein location and quantity, and thus it can be concluded that endogenous HDAC3 activity and HDAC3 protein location and quantity are unaffected in the absence of IRBP. Additionally, through immunofluorescence, it was concluded that H3k9me3 expression is unaffected by the absence of IRBP as well, and that there are no significant changes in this specific methylation expression between P5 and P36 in both C57 and IRBP KO mice.

As this current study presents the first trial of TSA injections on IRBP KO mice, it was opted to first use older mice that are more robust to handle a foreign drug. P40 mice were used, and pre/post injection ERGs and whole-eye biometry imaging was conducted. It was observed that in TSA injected mice, TSA caused no significant change in retinal thickness and total axial

length. Additionally, there was a slight decrease in visual function following TSA injection. From these experiments it can be concluded that at a dose of 2.5mg/kg over an injection period of 5 days, TSA has no significant affect against RD and myopia in a stable myopic model.

Although TSA cannot rescue function in a severely myopic mouse model, it still could prove to work in a preventative manner, as has been seen in other mouse models (Kitano et al., 2010). Thus, we injected P7 IRBP KO mice with TSA (1mg/kg) or vehicle (5% DMSO) over the course of 7 days—this injection point was chosen as we begin to see retinal thinning in IRBP KO mice around P8 which precedes retinal degeneration—as the size and shape of the eye is changing in IRBP KO mice, the larger eye in the KO causes the same volume of retina to be spread thinner over a larger surface area. Injection with TSA throughout this period of photoreceptor apoptosis could possibly slow or prevent the amount of cell death. However, there is no statistically significant difference in morphology between TSA and vehicle injected IRBP KO mouse. It is important to note that DMSO may be having a neuroprotective effect, as both the TSA and the vehicle (5% DMSO) injected experimental groups experienced a reduction in eyeball lengthening in comparison to the non-injected. This may indicate that a substitute vehicle should be selected to better isolated the mechanism TSA has in the eye. It additionally correlates with previous studies in other RD models that have shown DMSO has a protective effect (Sellers et al., 2014). Additionally, no functional improvement could be seen in the TSA injected mice compared to both vehicle injected and non-injected IRBP KO mice via ERGs. This lack of differences between experimental groups, however, could have been affected by the long period of time that took place between the last injection and then data collection (about 55 days). During this time, the retina could have reverted back to a severely degenerative and myopic state, even if it did experience improvement immediately following injections. To address this, I am

currently conducting an experiment where I am injecting IRBP KO mice with TSA (1.5mg/kg) or vehicle (5% DMSO) from P8-P25 intraperitoneally every other day and collecting whole-eye biometry and ERG data in the days immediately following the last injection.

This study also presents the first trial of VPA injections in IRBP KO mice. Again, older mice underwent injections first in order to establish a safe and effective drug dosage, especially as VPA is much more toxic than TSA. P40 IRBP KO mice were injected with either VPA (350mg/kg) or vehicle (1XPBS) over the course of 5 days intraperitoneally. Both pre and post morphological and function data was collected, and through biometry and ERG, it was revealed that, like TSA, VPA caused no significant changes in retinal thickness, total axial length, or retinal function. It can be concluded that at a dose of 350mg/kg over an injection period of 5 days, VPA has no significant affect against RD and myopia in a stable myopic and retinal degenerative model.

Much more research is required to truly understand what effect the HDAC inhibitors have on myopia and retinal degeneration. Regarding future experiments, we aim to focus on three areas. First, we plan to test a longer period of TSA injection in P40 IRBP KO mice. This is due to the fact that there was no elongation of the eye or thinning of the retina post TSA injection, so it could be possible that TSA, although it cannot completely save retinal function, it can stop further progression of phenotypical degradation, which is also an important topic to consider. Additionally, we aim to independently test the effect of TSA on myopia development in IRBP KO mice by treatment during P1-P7, as this age range is prior to eye elongation—it is a time window when retinoblasts divide for the first time and then undergo terminal differentiation. We also aim to independently test the effects of TSA on RD development with treatment from P8 and onwards, as retinal thinning becomes obvious by P15. This last objective, as mentioned, is

currently being addressed in my most recent experiment. In previous studies, TSA has been portrayed as mainly a more preventative drug. Therefore, we wish to see if TSA acts preventatively in a myopic or retinal degeneration model as well. Additionally, experiments involving VPA should be repeated as well to confidently determine if VPA has any beneficial effects, and whether or not VPA could be used as a viable therapeutic agent.

Overall, the current study presses deep to understand the relationship between epigenetics and myopia/RD, two fields that have been understudied so far. It is becoming clearer that our epigenome is just as important, if not more important, than our genome, and understanding the intricacies and regulations of specific epigenetic profiles is crucial for understanding disease development. As the prevalence of myopia is growing at an alarming rate, it is important to find solutions to vision loss that are not invasive (such as sub-retinal injections or LASIK), non-imposing (such as contacts or glasses), and effective in small quantities. As degeneration of visual acuity is inevitable in every individual, it is imperative that scientists better understand the underlying developmental mechanisms of myopia and retinal degeneration so that preventative and therapeutic treatments can quickly be identified.

Methods

Mouse husbandry

Mouse care and handling were approved by the Emory University Institutional Animal Care and Use Committee and adhered to standards recommended by the Association for Research in Vision and Ophthalmology (ARVO) and the Association for Assessment and Accreditation of Laboratory Animal Care (AAALAC). C57BL/6J (C57 WT) and congenic IRBP KO mice were used that had been backcrossed more than ten times to C57 WT. The C57 WT and IRBP KO mice colony is routinely screened for the *Crb1*$^{rd8/rd8}$ (rd8) mutation. The C57 WT and IRBP KO

mice used in the current study showed the absence of the rd8 mutation. The Emory University Division of Animal Resources housed and managed mice. Mice were housed at 23 °C on a 12 h:12 h light-dark Cycle and were given and standard mouse chow (Lab Diet 5001; PMI Nutrition Inc., LLC, Brentwood, MO) and water ad libitum.

TSA Injection

IRBP KO mice and C57 mice were randomly be assigned to experimental and control groups. Mice were injected daily from P40-P45 with TSA (2.5mg/kg in 10% DMSO solution; Catalogue number: T8552-1MG; Sigma-Aldrich, St. Louis, MO) or vehicle (DMSO) intraperitoneally using a double-blind system (Figure 2A). TSA dosage has been selected based on published data in mouse models (Kitano et al., 2010). Separate IRBP KO and C57 mice were injected with TSA (1mg/kg) or vehicle (5% DMSO) from P7-P14 (n=4). Additionally, a one-time injection of TSA (2.5mg/kg) was given to C57 P15 mice (n=5) to confirm the entry of TSA into the ocular space. Murine retinas were isolated 2 hours following injection (n=3) or 4 hours following injections (n=2). Murine retinas of non-injected age-matched mice were isolated as well (n=2). Retina proteins were isolated and used for HDAC enzymatic activity analysis. Mice were observed daily to monitor health and phenotypic changes.

VPA injection

IRBP KO mice and C57 mice were randomly be assigned to experimental and control groups. Mice were injected daily from P40-P45 with VPA (350 mg/kg in 1XPBS; Catalogue number: P4543-25G; Sigma-Aldrich, St. Louise, MO) or vehicle (1XPBS) intraperitoneally using a double-blind system (Figure 2B). VPA dosage has been selected based on published data in mouse models. Mice were observed daily to monitor health and phenotypic changes.

Whole-eye biometry

Following injections, mice were subjected to *in vivo* whole-eye biometrical imaging using a Bioptigen R4310 deep imaging SD-OCT system (Leica Microsystems, Durham, NC). Post-imaging analysis included measurement of the following parameters: central corneal thickness (CCT), anterior chamber depth (ACD), lens thickness (LT), vitreous chamber depth (VCD), retinal thickness (RT), and total ocular axial length. The mean thickness (± standard deviation, SD) was recorded. Biometry data was collected both before and after injection of HDACi or vehicle. Mice were anesthetized with a 10mg/mL ketamine 1.5 mg/mL xylazine solution to undergo *in vivo* imaging. Eyes were dilated with Tropicamide (Akorn, Lake Forest, IL) for 2 minutes, and Refresh Tears (Allergan, Dublin, Ireland) were used to keep eyes moist during the duration of the procedure. Mice were given a reversal agent of 0.1 mg/mL antisedan, and eyes were kept hydrated during their recover with Genteal Lubricant Eye Gel (Novartis, Basel, Switzerland).

SD-OCT and fundoscopy

A Micron IV SD-OCT system and a fundus camera were used (Phoenix Research Labs, Pleasanton, CA) to analyze retinal morphology in the C57 WT and IRBP KO mice at P48 (C57 WT, n = 2; KO, n = 4) and P78 (C57 WT, n = 2; KO, n = 4). Image-guided OCT images were obtained for the left and right eyes after a sharp and clear image of the fundus (with the optic nerve centered) was obtained. SD-OCT was a circular scan about 100 μm from the optic nerve head. Fifty scans were averaged. The retinal layers (indicated on the figure images) were identified according to published nomenclature (Dysli et al., 2015). Mice were anesthetized in the same manner they were when undergoing whole-eye biometry. Total retinal thickness and photoreceptor layer thickness were analyzed via Photoshop.

Electroretinography

An electroretinography system was used to analyze retinal function in the C57 WT and IRBP KO mice. The ground needle electrode was placed in the mouse's tail, and reference needle electrodes were placed on both cheeks of the mouse. Electrodes with DTL fiber were placed on the cornea and scotopic and photopic A and B wave amplitudes were recorded for the left and right eye. Each eye was subjected to five flash intervals of increasing intensity while dark adapted, then light adapted for 10 minutes. Each eye was then subjected to seven flash intervals of increasing intensity while light adapted. ERGs were collected both before and after injection of TSA, VPA or their respective vehicle. Mice were anesthetized with a 10mg/mL ketamine 1.5 mg/mL xylazine solution to undergo *in vivo* imaging. Eyes were dilated with Tropicamide (Akorn, Lake Forest, IL) for 2 minutes, Proparacaine (Akorn, Lake Forest, IL) was administered to numb the cornea, and Refresh Tears (Allergan, Dublin, Ireland) were used to keep eyes moist during the duration of the procedure. Mice were given a reversal agent of 0.1 mg/mL antisedan, and eyes were kept hydrated during their recover with Genteal Lubricant Eye Gel (Novartis, Basel, Switzerland).

Western Blot Analysis

Retinas from experimental C57 and IRBP KO rodent eyes were dissected from the RPE-choroid, homogenized, and lysed in RIPA Buffer Solution (Catalog number: R3792, Teknova; Hollister, CA). 1 tablet of protease inhibitor (Catalogue number: 11836153001; Sigma-Aldrich, St. Louise, MO) and 1 tablet of phosphatase inhibitor (Catalogue number: 4906837001; Sigma-Aldrich, St. Lousie, MO) per 10 mL were added to the lysis buffer before use to reduce proteolysis and maintain protein phosphorylation. The cellular debris was removed by low speed centrifugation (3000 rpm for 5 minutes) and protein concentrations of supernatants were determined by Pierce BCA Protein Assay Kit (Life Technologies Corporation, Grand Island, NY). Protein samples

were separated by SDS 4–15% Criterion TGX Stain-Free Gels (Biorad; Hercules, CA) transferred onto Polyvinylidene difluoride membranes that were blocked in blocking buffer (5% nonfat dry milk in phosphate- buffered saline and 0.1% Tween 20) for 1 hour at room temperature, incubated with primary antibody overnight at 4C, washed, incubated with horse radish peroxidase-conjugated secondary antibody for 2 hours at room temperature, developed with Luminata Crescendo Western HRP substrate, and image captured digitally. Densitometry measurements were performed using Image J software.

HDAC activity enzyme assay

Isolated C57 and IRBP KO murine retina proteins (following the same extraction protocol defined in the western blot analysis section) were used to asses HDAC3 enzymatic activity following the protocol contained in the Histone Deacetylase 3 (HDAC3) Activity Assay Kit (Catalogue number: EPI004-1KT; Sigma-Aldrich, St. Louise, MO). A protein concentration of 1.0 ug/mL was used in each enzymatic reaction. Both negative (addition of HDACi TSA) and positive controls (HDAC3 substrate) were included in each assay, and a standard 10 μM AFC (7-amino-4-trifluoromethyl coumarin) curve was used for statistical analysis. One unit is defined as the amount of HDAC3 able to generate 1.0 pmol of AFC per minute at 37 °C when incubated with the HDAC3 Substrate (R-HK-K(Ac)-AFC).

Immunohistochemistry and histology

Routine paraffin-embedded histology with hematoxylin and eosin (H&E) staining, plastic sectioning, staining with toluidine blue, and morphometric measurements were conducted as previously described (Wisard et al., 2011). C57BL/6J wildtype and IRBP KO/KO murine eyes were sectioned for immunohistochemistry staining with anti-HDAC3 antibody or collected for retinal protein isolation for western blot or enzymatic activity analysis.

Rigor, reproducibility, and transparency

All experiments will adhere to the rigor and reproducibility guidelines and principles set by the National Institutes of Health (NIH) (https://www.nih.gov/research-training/rigor-reproducibility).

References

1. Chen, J., & Qu, J. (2012). Experimental murine myopia induces collagen type I Ia1 (COL1A1) DNA methylation and altered COL1A1 messenger RNA expression in sclera. *Molecular Vision,* **18,** 1312-1324.
2. Chen, K., His, E., Hu, C., Chou, W., Liang, C., & Juo, S.H. (2012) MicroRNA-328 may influence myopia development by mediating the PAX6 gene. *Investigative Ophthalmology & Visual Science*, **53**, 2732-2739.
3. Clemson, CM., Tzekov, R., Krebs, M., Checchi, JM., Bigelow, C., & Kaushal, S. (2009) Therapeutic potential of valproic acid for retinitis pigmentosa. *British Journal of Ophthalmology*, **10**, 1136.
4. Crosson, C.E., Mani, S.K., Husain, S., Alsarraf, O., & Menick, D.R. (2010) Inhibition of histone deacetylase protects the retina from ischemic injury. *Investigative Ophthalmology & Visual Science*, **51**, 3639-3645.
5. *Dolgon, E. (2015) The myopia boom. Nature, **519**, 276-278.*
6. Dysli C, Enzmann V, Sznitman R, Zinkernagel MS. (2015) Quantitative Analysis of Mouse Retinal Layers Using Automated Segmentation of Spectral Domain Optical Coherence Tomography Images. *Transl Vis Sci Technol*, **4**, 9.

7. Hornbeak, D.M., & Young, T.L. (2009) Myopia genetics: a review of current research and emerging trends. *Current Opinion in Ophthalmology,* **20**, 356-362.

8. Kimura, A., Guo, X., Noro, T., Harada, C., Tanaka, K., Namekata, K., & Harada, T. (2015) Valproic acid prevents retinal degeneration in a murine model of normal tension glaucoma. *Neuroscience Letters*, **588**, 108-113.

9. Kitano, A., Okada, Y., Yamanka, O., Shirai, K., Mohan, R.R., & Saika, S. (2010) Therapeutic potential of Trichostatin A to control inflammatory and fibrogenic disorders of the ocular surface. *Molecular Vision*, **16**, 2964-2973.

10. Leo, S.W. (2017) Current approaches to myopia control. *Current Opinion in Ophthalmology*, **28**, 267-275.

11. Markand, S., Baskin, N.L., Chakraborty, R., Landis, E., Wetzstein, S.A., Donaldson, K.J., Priyadarshani, P., Alderson, S.E., Sidhu, C.S., Boatright, J.H., Iuvone, P.M., Pardue, M.T., & Nickerson, J.M. (2016) IRBP deficiency permits precocious ocular development and myopia. *Molecular Vision*, **22**, 1291-1308.

12. Mitton, K., Gzuzman, A., Deshpande, M., Byrd, D., DeLooff, C., Mkoyan, K., Zlojutro, P., Wallace, A., Metcalf, B., Laux, K., Sotzen, J., & Tran, T. (2014) Different effects of valproic acid on photoreceptor loss in Rd1 and Rd10 retinal degeneration mice. *Molecular Vision*, **20**, 1527-1544.

13. Mottamal, M., Zheng, S., Huang, T.L., & Wang, G. (2015) Histone deacetylase inhibitors in clinical studies as templates for new anticancer agents. *Molecules*, **20**, 3898-3941.

14. Pepperberg, D. R., Okajima, T. I. L., Wiggert, B., Ripps, H., Crouch, R. K., & Chader, G. J. (1993). Interphotoreceptor retinoid-binding protein (IRBP). *Molecular Neurobiology*, **7**, 61-84.

15. Sancho-Pelluz, J., Alavi, M.V., Sahaboglu, A., Kustermann, S., Farinelli, P., Azadi, S., van Veen, T., Romero, F.J., Paquet-Durand, F., & Ekstrom, P. (2010) Excessive HDAC activation is critical for neurodegeneration in the rd1 mouse. *Cell Death & Disease,* **1**, 24.

16. Sellers, J., Foster SL., Chrenek, MA., Iuvone, PM., & Boatright, JH. (2014) DMSO protects against light-induced retinal degeneration, yet increases tyrosine nitration. *Investigative Ophthalmology & Visual Science*, **55**, 2351.

17. Wisard, J., Faulkner, A,. Chrenek, MA., Waxweiler, T., Waxweiler, W., Donmoyer, C., Liou, GI., Craft, CM., Schmid, GF., Boatright, JH., Pardue, MT., & Nickerson JM. (2011) Exaggerated eye growth in IRBP-deficient mice in early development. *Investigative Ophthalmology &amp. Visual Science,* **52**, 5804–5811.

18. Wu, P., Huang, H., Yu, H., Fang, P., & Chen, C. (2016). Epidemiology of Myopia. *Asia-Pacific Journal of Ophthalmology*, **5**, 386-393.

19. Zhou, X., Ji, F., An, J., Zhao, F., Shi, F., Huang, F., Li, Y., Jiao, S., Yan, D., Chen, X., Chen, J., & Qu, J. (2012). Experimental murine myopia induces collagen type I Ia1 (COL1A1) DNA methylation and altered COL1A1 messenger RNA expression in sclera. *Molecular Vision,* **18,** 1312-1324.

Figure 1 :

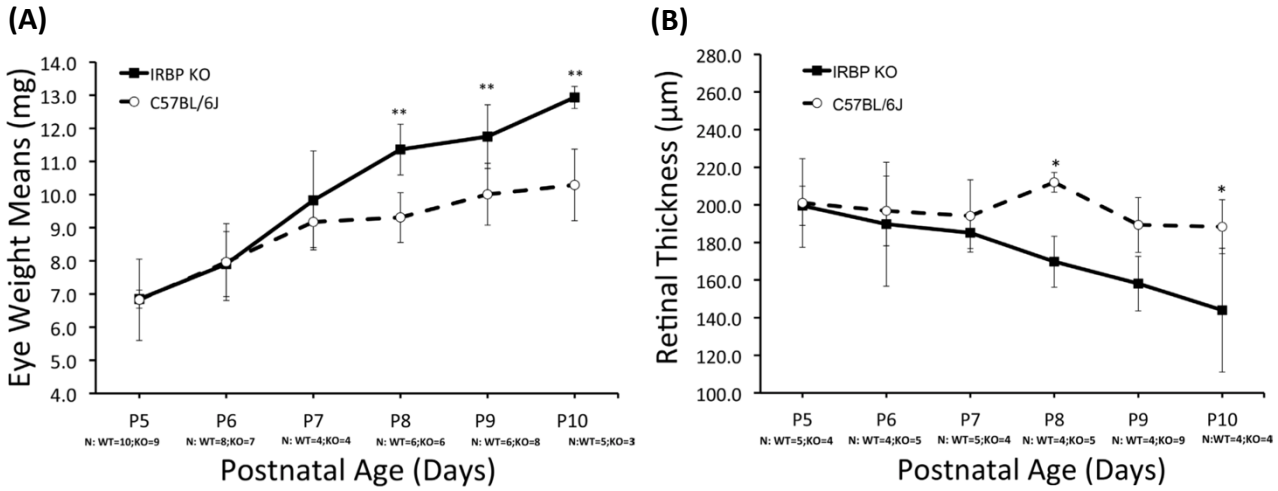

Figure 1. (A) Initiation of abnormal eye size in IRBP KO mouse. Eye weight of IRBP KO mouse started to increase in comparison to C57 WT mouse at P7, before eye opening. **(B)** Retinal thickness deviation in IRBP KO mouse. The retinal thickness of IRBP KO mice was thinner than C57 WT mice from P7 and later. Thickness difference becomes significant by P8 (Markand et al., 2016).

Figure 2:

(A)

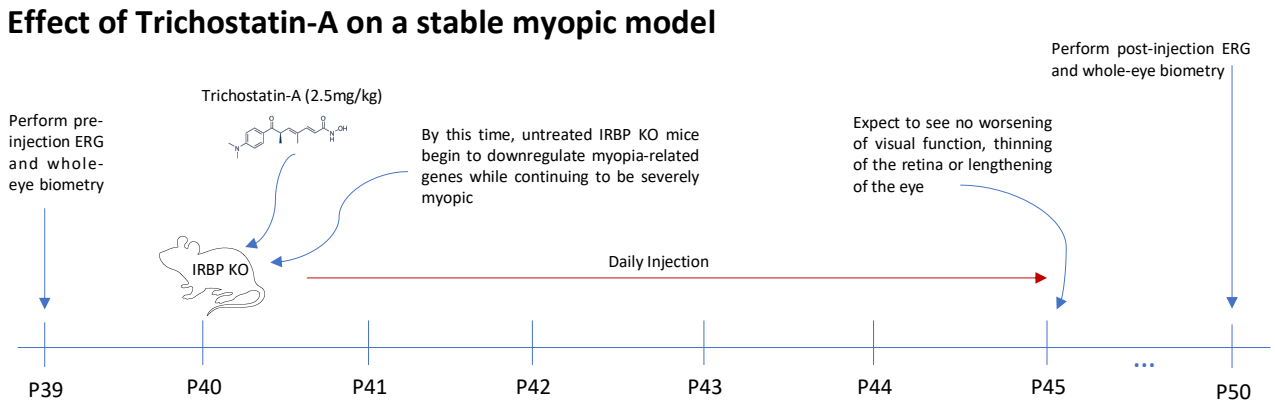

(B)

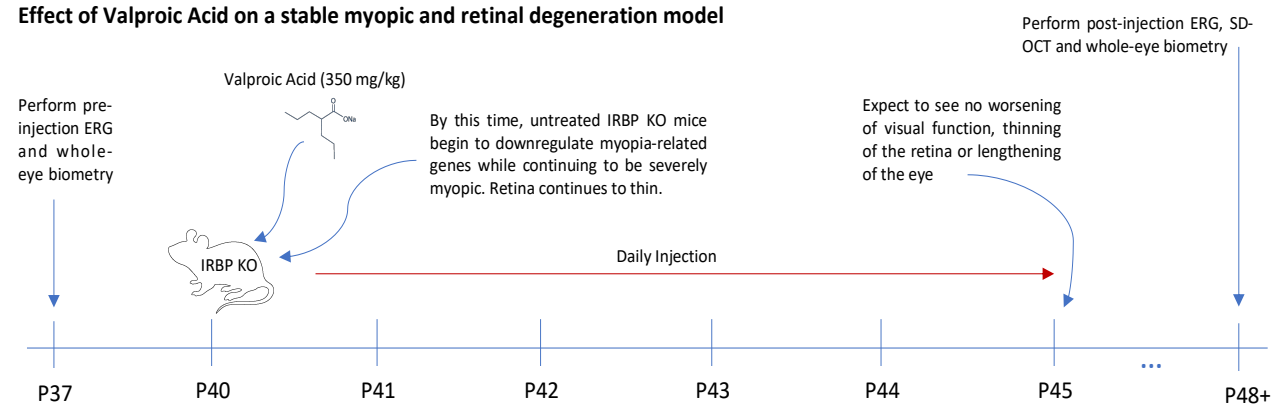

Figure 2. (A) Model of TSA injection timeline. Outlines dosage, period of injection, expected results and experiments performed to assess drug efficacy. Prior to each injection and experiment, whole-body length and whole-body weight measurements were taken. Eye were additionally harvested in some cases for destructive analyses. **(B)** Model of VPA injection timeline. Outlines dosage, period of injection, expected results and experiments performed to assess drug efficacy. Prior to each injection and experiment, whole-body length and whole-body weight measurements were taken. Eye were additionally harvested in some cases for destructive analyses.

Figure 3:

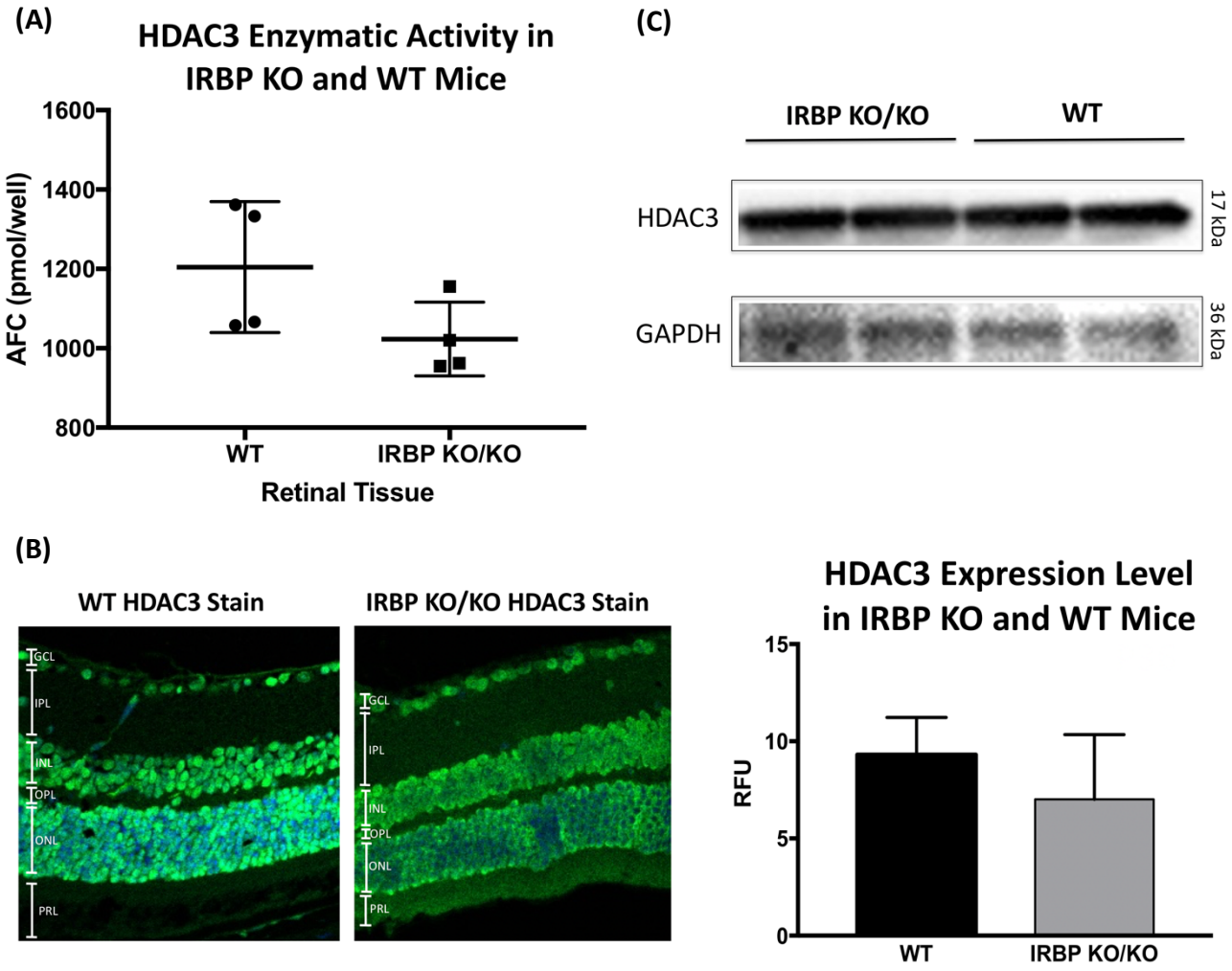

Figure 3. (A) Retinal tissue samples were prepared from P36 IRBP KO mice and P36 C57 WT control mice (n=4). An HDAC3 enzymatic activity assay was performed on the samples, yielding no statistically significant differences in HDAC3 activity between the two strains (paired t-test, α= 0.05, standard deviation (SD) shown). Each data point represents a different mouse. **(B)** Immunohistochemistry was conducted on IRBP KO and C57 WT (n=3) control sections (blue = DAPI; green = HDAC3. Retinal segments can be seen labeled in white. Quantification is shown on the right, and no obvious differences can be observed in fluorescence intensity between IRBP KO and C57 WT sections (unpaired t-test, α= 0.05, SD shown). **(C)** A western blot using IRBP KO and C57 WT retinal samples was performed to show that there was no noticeable difference in HDAC3 protein quantity.

Figure 4:

(A)

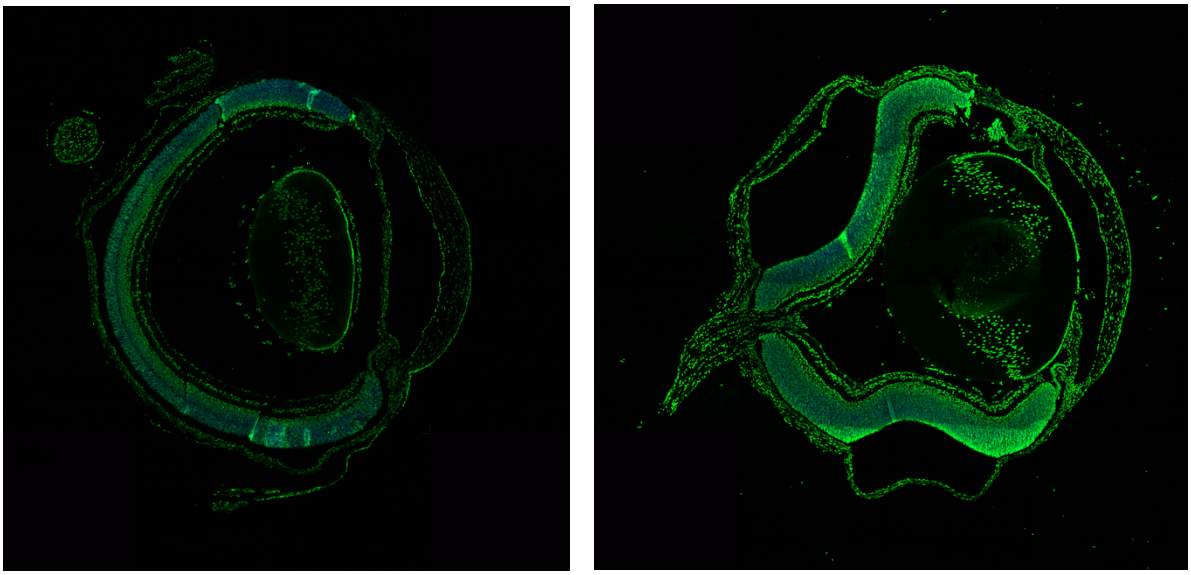

P5 IRBO KO **P5 C57**

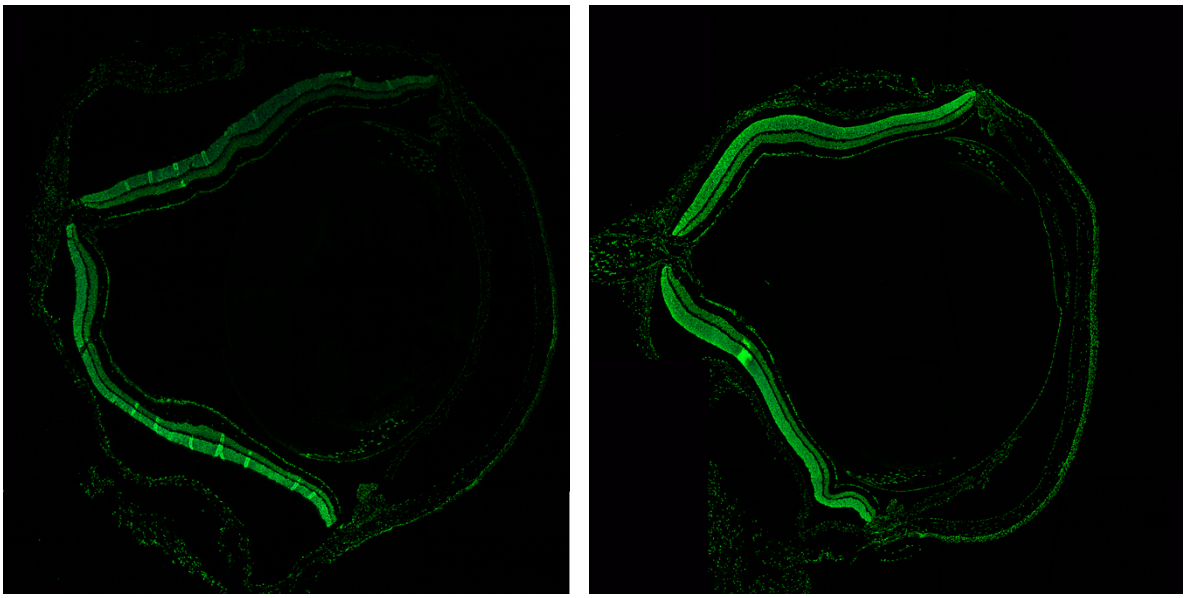

P36 IRBO KO **P36 C57**

Figure 4. (A) Immunohistochemistry was conducted on P5 IRBP KO and C57 eye sections (blue = DAPI, green = H3k9me^3). Common histone methylation modifications were stained for, one of which was H3k9me^3 (shown). Fluorescence quantification showed no significant differences between IRBP KO/KO and C57 samples at either age (ex. comparing P5 IRBP KO/KO and C57 samples). **(B)** P36 IRBP KO and C57 samples were sectioned and stained for H3k9me^3 in the same matter as (A). There were there significant differences between ages regarding the presence H3k9me^3 in retinal tissue (ex. comparing P5 and P36 IRBP KO/KO samples).

Figure 5:

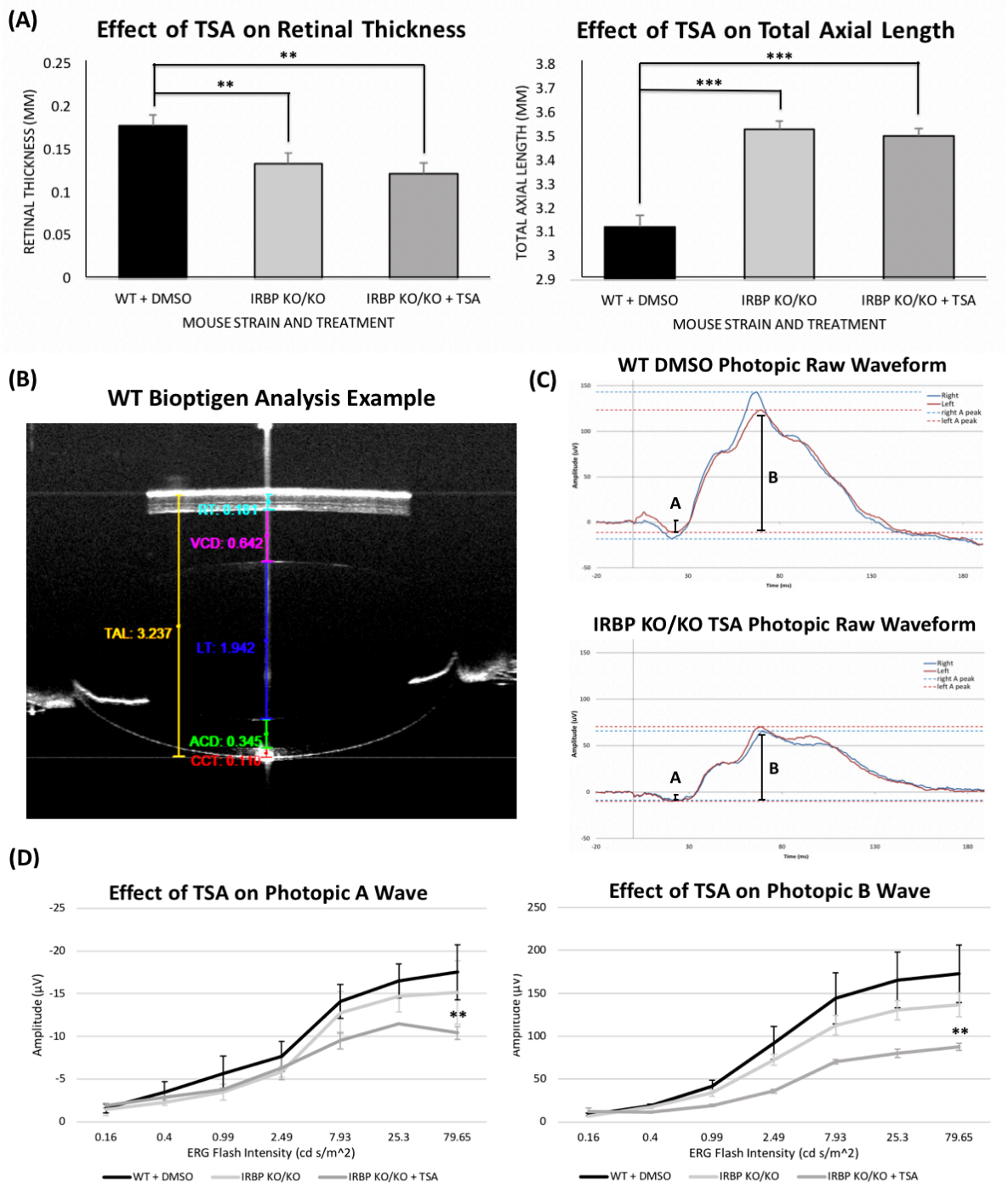

Figure 5. (A) Whole-eye biometry was performed on IRBP KO/KO (n=4) and C57 WT (n=4) pre and post TSA or vehicle injection (P39 and P50, respectively). There was no significant difference in either total axial length or retinal thickness following treatment of TSA in IRBP KO mice (paired t-test, α= 0.05, SD shown). **(B)** Example of whole-eye biometry analysis. **(C)** Example photopic raw waveforms from IRBP KO/KO + TSA and C57 WT +DMSO treated mice at a flash intensity of 79.65 cd s/m^2. Mice were light-adapted for 10 minutes and cone response was measured via full-flash (photopic shown) and flicker ERG. **(D)** TSA was not preventative of cone-driven vision loss in IRBP KO/KO mice. Both photoreceptors (a-wave) and ON bipolar cells (b-wave) continued to decrease in function despite treatment with TSA. (unpaired t-test between C57 WT and IRBP KO/KO groups, α= 0.05). Paired t-tests (α= 0.05, SD shown) revealed no significance between differences in IRBP KO/KO and IRBP KO/KO + TSA conditions.

Figure 6:

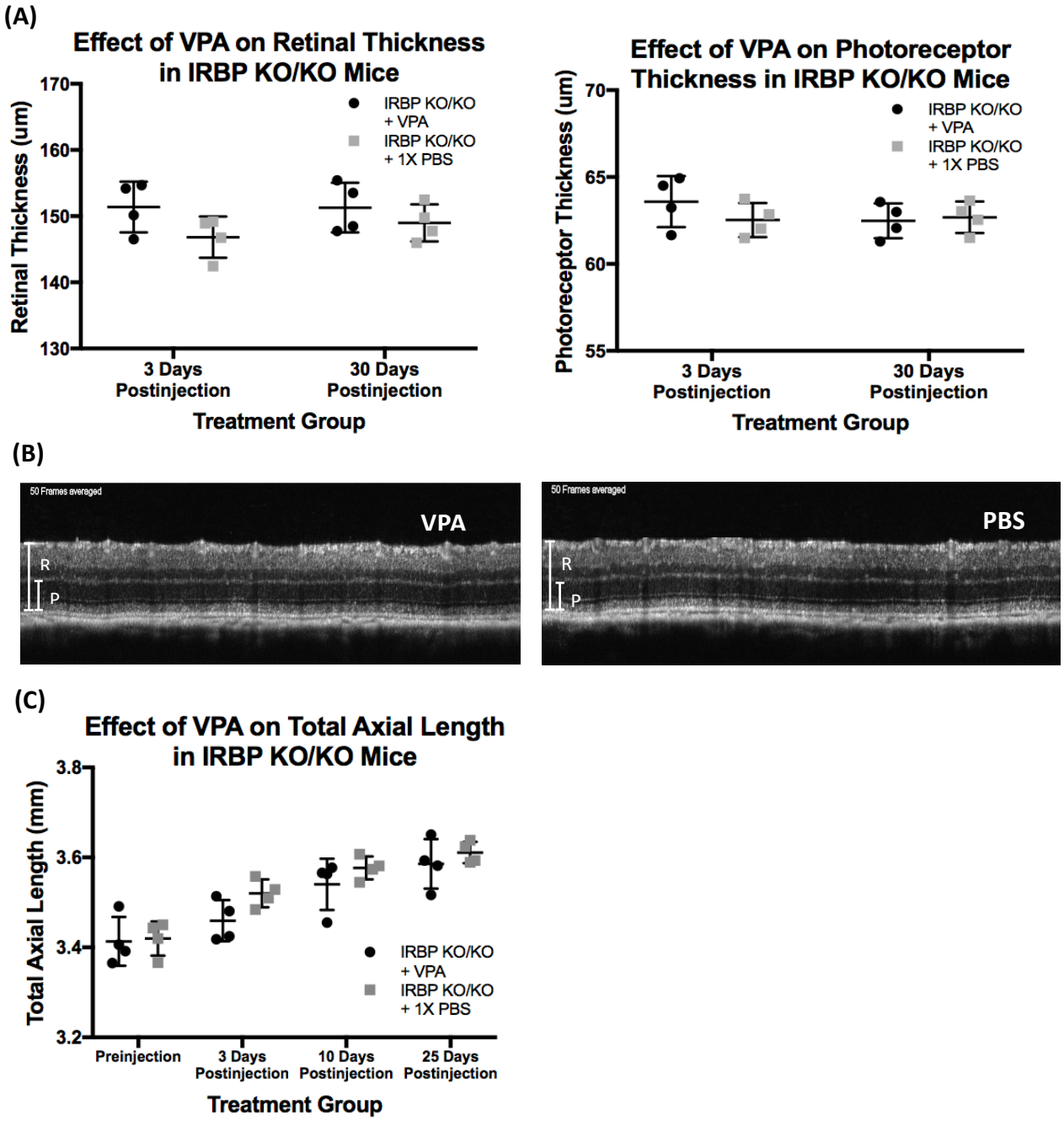

Figure 6. (A) SD-OCT was performed on IRBP KO/KO (n=4) post VPA or vehicle injection. There was no significant difference in either retinal thickness or photoreceptor thickness following treatment of TSA in IRBP KO mice both following 3 days after injection or 30 days after injection between VPA or vehicle injected mice (unpaired t-test, α= 0.05, SD shown). Each point represents a different mouse. **(B)** Example of SD-OCT images of retina obtained from VPA or vehicle injected IRBP KO mice (R = retinal thickness, P = photoreceptor thickness). A VPA treated retina on the left and a vehicle (PBS) treated retina on the right. No clear difference can be seen between the two retinas visually. **(C)** Whole-eye biometry was performed on IRBP KO/KO mice (n=4) both before and after injection of either VPA or vehicle at pre-injection, 3 days post-injection, 10 days post injection, and 25 days post injection. Each point was a different mouse. There was no significant difference in total axial length following treatment of VPA in IRBP KO mice (two-way ANOVA, α= 0.05, SD shown).

(D)

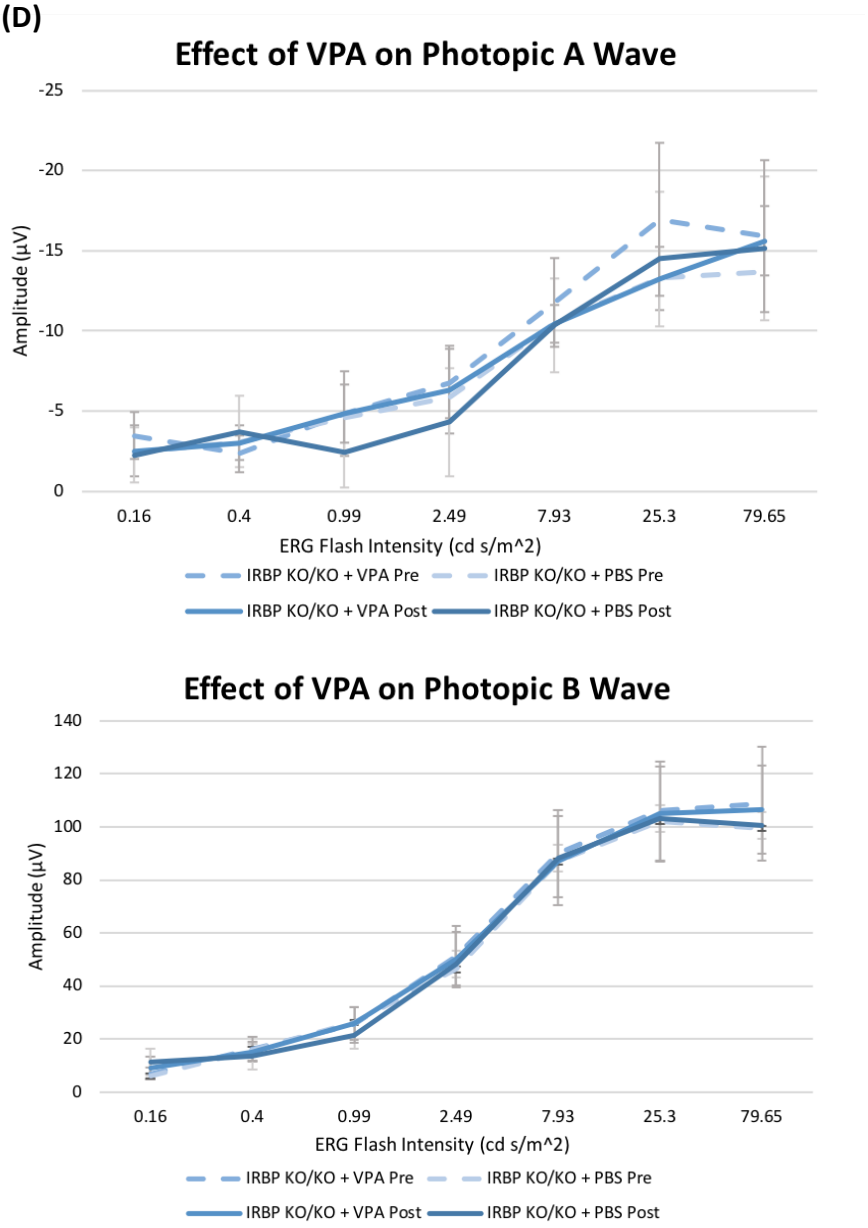

Figure 6. (D) Pre and post injection data was collected at P37 (shown as pre), P48, and P58 (shown as post) on treated IRBP KO/KO mice (n=4). VPA was not preventative of cone-driven vision loss in IRBP KO/KO mice. Both photoreceptors (a-wave) and ON bipolar cells (b-wave) showed no decrease in function following treatment (unpaired t-test, α= 0.05, SD shown), regardless of whether receiving VPA or vehicle.

Figure 7:

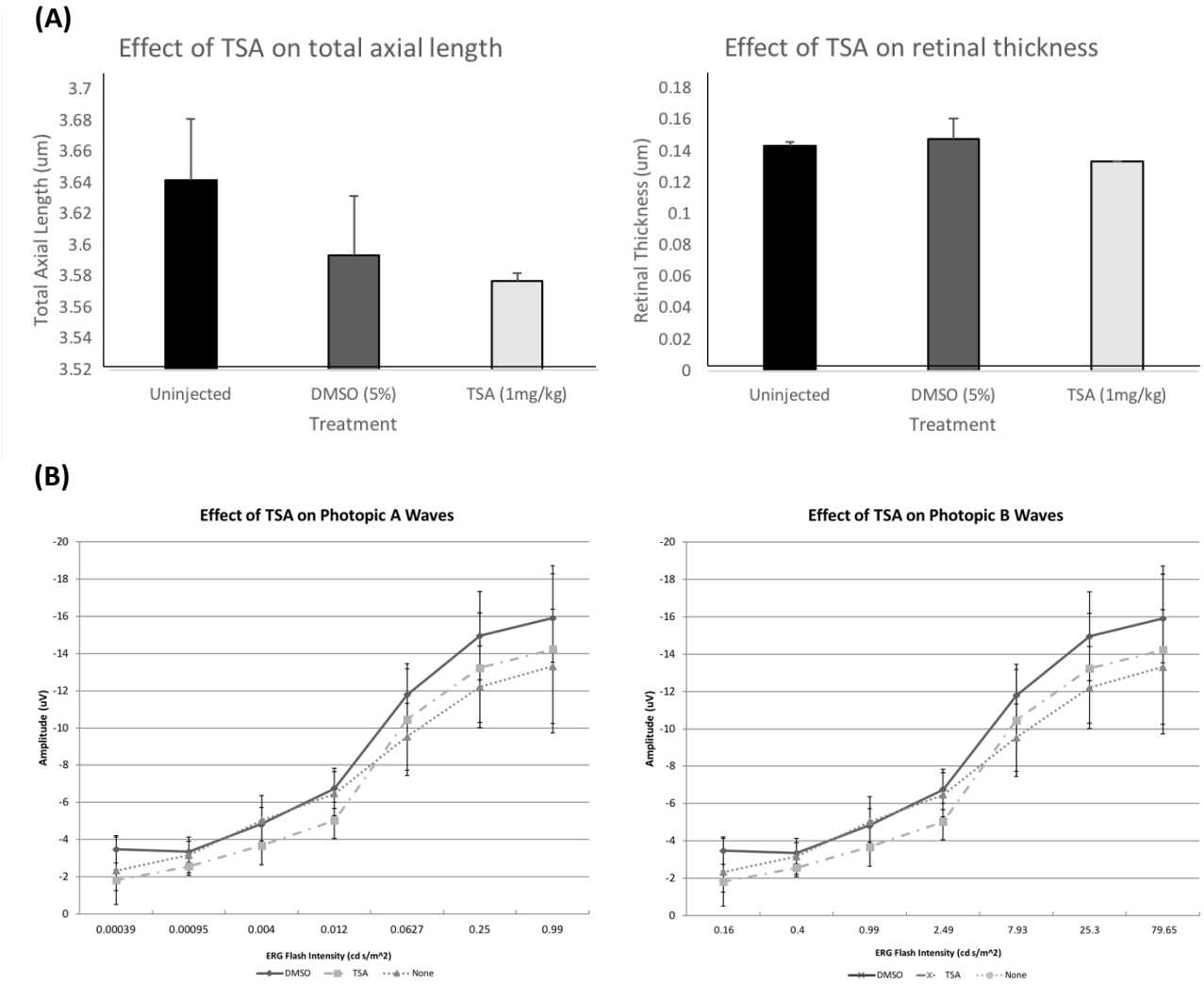

Figure 7. (A) Whole-eye biometry data was collected post-injection of P70 IRBP KO mice: non-injected (n=2), vehicle injected (n=2), and TSA injected (n=3). Total axial length and retinal thickness were among measurements collected via *in vivo* imaging. No statistical significant differences were observed between the three groups for either morphological measurement (one-way ANOVA, α= 0.05, SD shown). **(B)** ERG data was collected on P70 IRBP KO mice (non-injected (none) = dotted, TSA injected. = dashed, vehicle injected (5% DMSO) = solid). No statistical differences could be seen at any flash point between any treatment group in either photopic A or B waveforms.